Model experiments for direct visualization of grain boundary deformation in nanocrystalline metals

Krystyn J. Van Vliet,[a] Sedina Tsikata, and Subra Suresh
Department of Materials Science and Engineering, Massachusetts Institute of Technology, Cambridge, Massachusetts 02139

(Received 10 January 2003; accepted 2 June 2003)

Recent experimental studies on nanocrystalline metals have shown that mechanical strength may decrease with decreasing grain size d for $d<10-15$ nm. The mechanisms underlying this trend are not understood, although such a relationship is in distinct contrast to that seen in microcrystalline metals whereby strength increases with decreasing grain size. Here, we present direct experimental observations of deformation via the bubble raft model, a two-dimensional analog to fcc crystals. We adopt nanoindentation as a means to introduce localized deformation, and quantify critical conditions for defect nucleation. We identify a transitional d of approximately 7 nm, at which further grain refinement leads to a decrease in the stress required to initiate plastic deformation. Further, we observe a concurrent transition in the primary deformation mechanism from discrete dislocation emission from grain boundaries ($d>7$ nm) to localized grain boundary migration ($d<7$ nm). Thus, these data suggest that both the onset and mechanisms of plasticity in nanocrystalline materials change markedly below a critical grain size. © *2003 American Institute of Physics.* [DOI: 10.1063/1.1597417]

The connection between a characteristic microstructural length scale, average grain size d, the yield strength σ_y, and fracture strength of metals was elucidated by Hall[1] and Petch[2] as

$$\sigma_y = \sigma_{yo} + k_y d^{-1/2}, \tag{1}$$

where σ_{yo} is the friction stress required to move a dislocation and k_y is a material-dependent intensity factor related to the hardening of grain boundaries. The Hall–Petch (HP) relation has been established experimentally[3,4] for $d>1$ μm.

Modification of processing methods has made possible the synthesis of metals with $d<100$ nm. As these materials are currently available in only small quantities, nanoindentation is the most common method to estimate σ_y as a function of d. (Measured indentation hardness H is proportional to σ_y.[5]) Equation (1) would imply increased strength and hardness when trends observed for microcrystalline metals are extrapolated down to the nanocrystalline regime, as reported for Cu with $d>10$ nm.[6] However, other experimental data in close-packed metals indicate an opposite relationship between σ_y and d for $d<10$ nm.[7–9] The validity of these latter results has been debated and ascribed to possible artifacts in material structure and characterization.[6,10,11] Thus, as both the strengthening trends and mechanisms thereof are open questions, we hereafter use the broad terms ''HP-type'' to denote increasing resistance to the onset of yielding with decreasing d, and ''reverse HP-type'' to denote decreasing resistance to the onset of yielding with decreasing d.

Atomistic computational simulations[12–14] were employed subsequently to simulate plastic deformation in fcc nanocrystalline metals. Although sample size and loading conditions in such computations can differ substantially from experimental parameters, these uniaxial simulations suggest a reverse HP-type effect for $d\sim 7-8$ nm in Ni and Cu, and researchers suggest mechanisms ranging from room temperature creep[14] to grain boundary sliding.[15]

A complementary approach to three-dimensional experiments and computations is *in situ* observation of deformation via the Bragg–Nye soap bubble raft model, an experimental analog to two-dimensional (2D) fcc crystals.[16] Recently, we have adapted this model for nanoindentation experiments in single crystal rafts to demonstrate and to validate analytical models of homogeneous nucleation of dislocations within a perfect crystal.[17–19] Here, we extend this concept to polycrystalline rafts to investigate the effect of d on the resistance to plastic deformation in 2D, model nanocrystals. A particular objective of the present work was to document and to visualize directly the mechanistic origins of possible transitions from strengthening to weakening with decreasing d.

The methods of bubble raft production[16] and single crystal raft construction[17] are reported elsewhere. Briefly, pressurized air is forced through a micropipette submerged in a glycerine-soap solution, resulting in uniformly sized bubbles of 1 mm diameter. The interaction of the bubbles is qualitatively similar to the interatomic (pair) potential of fcc metals (Cu, Ni) of ~ 0.3 nm atomic diameter.[20] This size scale analogy whereby 1 mm in real space represents 0.3 nm in atomistic space is assumed later. In the present experiments, nanocrystalline aggregates of $\sim 150\,000$ bubbles were constructed by aggregating many single crystal {111} rafts (grains). The boundary conditions of the ''nanocrystalline'' rafts are shown in Fig. 1(a). The average grain size d of a given raft was chosen to be a single value between 4 and 37 nm, varying $\leqslant 20\%$, as quantified via the line-intercept method on acquired images; new rafts were constructed for each d. This range of d simulates, in 2D, that attained through nanocrys-

[a]Author to whom correspondence should be addressed; present address: Department of Surgical Research, Children's Hospital and Harvard Medical School, Boston, MA 02115; electronic mail: krystyn@mit.edu

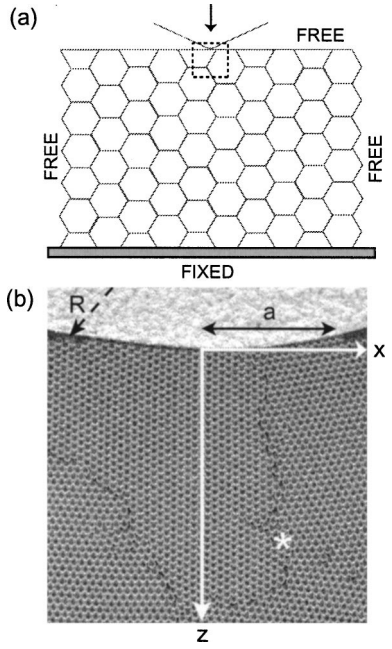

FIG. 1. (a) Schematic of raft boundary conditions, fixed against a rigid substrate (gray) along one edge and otherwise free to displace in-plane. Dotted box indicates region shown in (b). Nanocontact parameters include the in-plane coordinates (x,z) and contact half-width a for a constant indenter tip radius R of 28 nm.

talline metal processing methods.[21] The raft most closely approximates the as-prepared state of a real nanocrystal, as there was minimal structural relaxation of the raft upon aggregation of the individual grains. The aluminum indenter plate was machined to approximate in 2D the typical Berkovich geometry, with a tip radius R of 28 nm. Indentation proceeded in displacement control at a scaled velocity of 0.7 nm/s, until defect activity was observed. Nanoindentation of all nanocrystalline rafts induced defect nucleation from grain boundaries and grain boundary junctions, and no defect nucleation initiated from the grain interior. Defect formation was observed to proceed primarily from grain boundary triple junctions.

Several rationales for reverse HP-type trends posit that, at very small d, plastic deformation originates from and is accommodated solely by grain boundaries.[22] Thus, an important application of the nanocrystalline raft is determination of whether deformation stresses and mechanisms vary with d. The mean pressure p_m sustained by the raft can be calculated at the elastic limit, or the initiation of dislocation activity within the raft. As the load P per unit length is not well-defined in 2D indentation, p_m cannot be calculated as $P/[\pi a^2]$, where a is the half-width of contact. However, p_m can be inferred from the observed values a and R for a constant value of E via Hertzian (elastic) contact mechanics[23]

$$p_m = \frac{\pi}{4}\frac{aE}{2R} = \frac{\pi}{4}p_0 . \tag{2}$$

where p_0 is maximum pressure and E is the elastic modulus of the bubble raft for the present case of a rigid indenter. (As E in this 2D system is measured experimentally in units of [force]/[length], the units of p_m are also [force]/[length].)[16] The magnitude of this imposed pressure is important in that

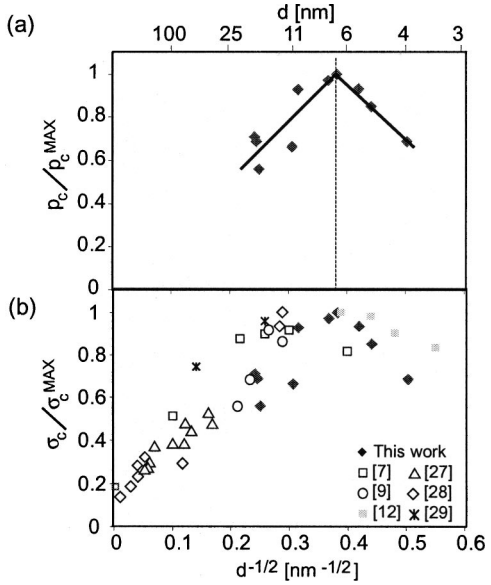

FIG. 2. (a) Nanoindentation of rafts of average grain size d ranging 4–37 nm. Critical mean pressure p_c, normalized by the maximum experimentally measured value, decreases with decreasing d for $d<7$ nm; (b) Comparison with experimental σ_y data for electrodeposited Ni shows a transitional d approximately equal to that indicated by the bubble raft experiments.

p_m is proportional to the resolved shear stress τ_{xz}^r.[23] The (unresolved) shear stress τ_{xz} at any point (x,z) inside an isotropic elastic solid can be determined analytically[24]

$$\tau_{xz} = -\frac{p_0}{a} n\left(\frac{m^2 - z^2}{m^2 + n^2}\right), \tag{3}$$

where m and n are polynomial functions of (x,z) and a. Thus, a decrease in p_m indicates a decrease in τ_{xz}^r. Here, the *critical* value of mean pressure p_c does not imply generalized plastic yielding, but rather indicates the magnitude of critical resolved shear stress required to induce defect activity locally in a polycrystalline aggregate: an important component of generalized yielding in nanocrystalline materials, where the volume fraction of grain boundaries can reach 50%. For all experiments, $R=28$ nm and the (x,z,a) configuration corresponding to the initial defect nucleation event was determined [see Fig. 1(b)], enabling calculation of p_c, p_0 and τ_{xz} according to Eqs. (2) and (3).

Figure 2(a) shows that p_c increases with decreasing average grain size for $d>7$ nm, consistent with HP-type behavior, but then decreases with decreasing grain size for $d<7$ nm. These data indicate that the magnitude of τ_{xz}^r sustainable by the nanocrystal is proportional to d for $d<7$ nm, and are consistent with computational atomistic results[12,13] and recent experimental results for close-packed metals [Ref. 8 and Fig. 2(b)].[27–29] These results can be compared quantitatively with those derived from single crystal {111} raft experiments with the same indenter tip radius R, where homogeneous defect nucleation occurs at a subsurface depth $z=0.78a$, the position of maximum $\tau_{xz}=0.30p_0$.[17] In the current experiments, we observed that the maximum τ_{xz} occurred for d of 13 nm and was only $0.23p_0$, representing a 23% decrease with respect to that required for the single crystal. In addition, the maximum p_c occurred for d of 6.8 nm, and was 7.4% less than that determined experimentally for the defect-free single crystal. These results confirm the

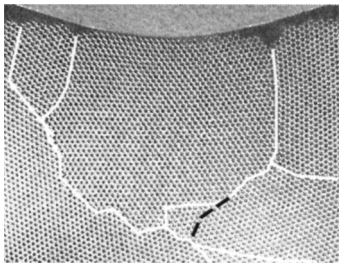

FIG. 3. Migration of grain boundary regions, observed primarily for $d < 7$ nm. Black dashed and solid white lines denote original and final position, respectively, of grain boundary region at triple junction.

intuitive expectation that the contact stress required to nucleate dislocations from the grain boundary is less than that required for homogeneous nucleation. These findings represent the experimental, quantitative measurement of the relative strength of grain boundaries in model nanocrystals, and complement recent atomistic computations on nanoindented Au where the p_c required to nucleate dislocations from a grain boundary can be as much as 18% less than that required for a single crystal.[25]

Defect activity was observed to occur in two distinct modes: discrete nucleation of individual dislocations (emission) and localized collective motion of a grain boundary region (migration). Nanocrystals of $d > 7$ nm primarily exhibited emission (Fig. 1 at *), whereas nanocrystals of $d < 7$ nm primarily exhibited migration (Fig. 3). Both deformation modes initiated most often at grain triple junctions, but were also observed at individual grain boundaries. Grain boundary migration proceeded by the collective motion of individual atoms and vacancies associated with the grain boundary region. This deformation mechanism is consistent with atomistic simulations for Ni and Cu, for which grain boundary sliding and subsequent migration were reported.[13] Although grain boundary sliding was quantified in the current study through image analysis of several experiments, no significant difference in the degree of motion as a function of d was observed.

We note that Eqs. (2) and (3) are formulations which assume elastic isotropy of a continuum; their application in this analysis is approximate in that it ignores length scales and anisotropies due to the presence of grain boundaries. In addition, although it can be argued that the disparate constraint of the bubbles between the soap solution (bottom) and ambient air (top) invalidates a 2D approximation, we note that all bubbles remained in-plane, and no bubbles popped, as a result of the large strain deformation imposed via indentation. A further limitation of these experiments is a lack of robust statistical analysis with respect to the various length scales present: Independent variation of grain size, grain boundary character, in-plane grain orientation, and grain boundary position with respect to the contact radius were difficult to achieve in the 24 experiments conducted in this study. Although the earlier results focus primarily on the role of d, the effect of other length scales is discussed elsewhere.[26]

From these experiments for $4\text{ nm} < d < 37$ nm, we observed several general features: (i) Defect activity initiated only from grain boundaries and grain boundary triple junctions. (ii) Critical mean pressure required to initiate defect activity increased with decreasing grain size for $d > 7$ nm (strengthening), but decreased with decreasing grain size for $d < 7$ nm (weakening). This response indicates a transition in the resolved shear stress required to initiate plastic deformation that correlates with grain size. (iii) In the strengthening regime, the primary deformation mechanism was discrete dislocation emission from grain boundary regions, whereas in the weakening regime, the primary deformation mechanism was grain boundary migration. (iv) Dislocation nucleation occurred under mean pressures which were at least 7% lower and at local shear stresses which were at least 23% lower than those required to nucleate defects via indentation in a perfect crystal. Although the experimental variability with respect to microstructural length scales makes it difficult to assess the statistical veracity of quantitative results such as the value of the transitional grain size d_{tr}, the qualitative finding—a grain size exists at which both the deformation mode and correlation with strength change—appears justified. These observations can guide systematic investigations, via both experiments and computations, of the unique response of grain boundaries in nanocrystalline metals.

[1] E. O. Hall, Proc. Phys. Soc. London, Sect. B **64**, 747 (1951).
[2] N. J. Petch, J. Iron Steel Inst., London **174**, 25 (1953).
[3] R. W. Armstrong, Adv. Mater. Res. (N.Y.) **4**, 101 (1970).
[4] M. A. Meyers and K. K. Chawla, *Mechanical Metallurgy* (Prentice Hall, Englewood Cliffs, NJ, 1984), p. 494.
[5] D. Tabor, *Hardness of Metals* (Oxford University Press, Oxford, 1951).
[6] P. G. Sanders, J. A. Eastman, and J. R. Weertman, Acta Mater. **45**, 4019 (1997).
[7] U. Erb, A. M. El-Sharik, G. Palumbo, and G. K. T. Aust, Nanostruct. Mater. **2**, 383 (1993).
[8] C. C. Koch, P. Fedkiw, and J. Narayan, *NSF Partnership in Nanotechnology Conference*, 29–30 Jan. 2001, Arlington, VA; J. Naryan, J. Nanopart. Res. **2**, 91 (2000).
[9] C. A. Schuh, T. G. Nieh, and T. Yamasaki, Scr. Mater. **46**, 735 (2002).
[10] G. E. Fougere, J. R. Weertman, R. W. Siegel, and S. Kim, Scr. Metall. Mater. **26**, 1879 (1992).
[11] R. A. Masumura, P. M. Hazzledine, and C. S. Pande, Acta Mater. **46**, 4527 (1998).
[12] J. Schiøtz, F. D. Di Tolla, and K. W. Jacobsen, Nature (London) **391**, 561 (1998).
[13] H. Van Swygenhoven, A. Caro, and D. Farkas, Scr. Mater. **44**, 1513 (2001).
[14] V. Yamakov, D. Wolf, S. R. Phillpot, and H. Gleiter, Acta Mater. **50**, 61 (2002).
[15] H. Van Swygenhoven, Science **296**, 66 (2002).
[16] W. L. Bragg and J. F. Nye, Proc. R. Soc. London, Ser. A **190**, 474 (1947).
[17] A. Gouldstone, K. J. Van Vliet, and S. Suresh, Nature (London) **411**, 656 (2001).
[18] J. Li, K. J. Van Vliet, T. Zhu, S. Yip, and S. Suresh, Nature (London) **418**, 307 (2002).
[19] K. J. Van Vliet, J. Li, T. Zhu, S. Yip, and S. Suresh, Phys. Rev. B **67**, 104105 (2003).
[20] W. M. Lomer, Proc. R. Soc. London, Ser. A **196**, 182 (1949).
[21] X. D. Liu, M. Nagumo, and M. Umemoto, Mater. Trans., JIM **101**, 1033 (1997).
[22] H. Van Swygenhoven, M. Spaczer, and A. Caro, Nanostruct. Mater. **10**, 819 (1998).
[23] K. L. Johnson, *Contact Mechanics* (Cambridge University Press, New York, 1985).
[24] E. McEwen, Philos. Mag. A **40**, 454 (1949).
[25] E. T. Lilleodden, J. A. Zimmerman, S. M. Foiles, and W. D. Nix, J. Mech. Phys. Solids **51**, 901 (2003).
[26] K. J. Van Vliet, Ph.d. thesis, Massachusetts Institute of Technology, 2002.
[27] F. Ebrahimi, G. R. Bourne, M. S. Kelly, and T. E. Matthews, Nanostruct. Mater. **11**, 343 (1999).
[28] G. D. Hughes, S. D. Smith, C. S. Pande, H. R. Johnson, and R. W. Armstrong, Scr. Metall. Mater. **20**, 93 (1986).
[29] C. Schuh (unpublished).